npj | urban sustainability

Article

Published in partnership with RMIT University

https://doi.org/10.1038/s42949-025-00202-2

Socially equitable climate risk management of urban heat

Check for updates

Michael Friesenecker [1,7], Antonia Schneider [2,7], Marianne Bügelmayer-Blaschek[3], Michael Getzner [2], Claudia Hahn[4], Martin Schneider[3], Sebastian Seebauer [5], Wojciech Zawadzki [6], Maja Zuvela-Aloise[4] & Thomas Thaler [1]

As the management of extreme weather events becomes increasingly important, climate adaptation strategies are paramount. However, current climate adaptation strategies often overlook aspects of social inequality or even risk exacerbating these. An example is the implementation of Nature-based Solutions (NbS). These approaches can result in green gentrification; the displacement and exclusion of marginalized groups due to increased attractiveness and value of nearby property. The consideration of social impacts into climate adaptation policies represents a significant challenge because climate policies are usually determined independently from social policies (policy siloing). Here we demonstrate a decision-making process that ensures socially equitable climate adaptation in an urban area. The proposed decision-making framework consists of three sequential stages: (1) climate risk assessment, (2) adaptation analysis, and (3) impact analysis. This decision-making method is applicable to cities worldwide. The City of Vienna, Austria and NbS are used to illustrate how climate adaptation policy can be integrated with social policy to achieve socially equitable urban heat risk management. We showcase that breaking current policy silos is necessary to achieve a socially equitable climate change adaptation strategy.

As temperatures globally rise at an unprecedented rate, the need to adapt to climate change has become part of mainstream planning and policy-making, particularly in urban regions[1,2]. Urban regions are especially affected by high and increasing summer temperatures caused by a combination of anthropogenic climate change and soil sealing[3–5]. The population of many urban areas around the world has grown and continues to grow due to employment opportunities, cultural diversity, improved infrastructure, and in developing countries especially because of the underdevelopment in rural areas[6]. However, if urbanization is accompanied by lack of blue and green spaces, it will exacerbate the negative impacts of a warmer climate, intensifying exposure and vulnerability[7–9].

Urban heat has become a major public health problem. It is associated with severe thermal discomfort and significant increases in mortality and morbidity rates, causing more casualties than other natural hazard events[10–12]. However, health risks are not equally distributed across society. In particular, children, the elderly, socially isolated individuals, people with pre-existing medical conditions and those with low incomes are typically more vulnerable to adverse health outcomes than others[13–15].

Higher health risks are not only a consequence of urbanization and climate change. They also depend on the ability of individuals and households to adapt to, and to cope with, heatwaves. Low-income residents in particular often struggle to adapt to extreme heat events. First, they often lack private green spaces and have high indoor temperatures due to poorly insulated or ventilated housing[15,16]. Second, low-income residents are unable to make or afford building adaptations, such as blinds or air conditioning[17]. Consequently, low-income residents are more dependent on the cooling function of public urban green and blue infrastructure[18–20].

In this regard, Nature-based Solutions (NbS), such as green roofs, green facades, greened streets, parks and water bodies have been proposed as effective means to mitigate the urban heat island effect[20,21]. The positive assessment of NbS extends to the preferences of citizens, who are strongly in favor of green and blue infrastructure to combat urban heat[22–25]. NbS also provide numerous co-benefits; increased biodiversity, aesthetic appeal, improved quality of public space and relieving pressure on the sewage system during heavy rainfall events[26,27]. Consequently, NbS have political and economic appeal. NbS can also be

[1]Institute of Landscape Planning, BOKU University, Vienna, Austria. [2]Department of Public Finance and Infrastructure Policy, TU Wien, Vienna, Austria. [3]AIT Austrian Institute of Technology, Vienna, Austria. [4]GeoSphere Austria – Federal Institute of Geology, Geophysics, Climatology and Meteorology, Vienna, Austria. [5]LIFE Institute for Climate, Energy Systems and Society, JOANNEUM RESEARCH Forschungsgesellschaft mbh, Graz, Austria. [6]Faculty of Economic Sciences, University of Warsaw, Warsaw, Poland. [7]These authors contributed equally: Michael Friesenecker, Antonia Schneider. e-mail: michael.friesenecker@boku.ac.at; antonia.schneider@tuwien.ac.at

integrated into existing infrastructure, are cost-effective in the long term, and durable compared to technical retrofits such as air conditioning systems[28].

Although typically presented as no-regret or win-win adaptation measures in climate change research[29], the implementation of NbS can lead to undesirable trade-offs and side effects. For instance, NbS can increase levels of pollen in the air or compete with other uses in public space[30]. However, the most common undesirable trade-offs arise when issues of social equity are overlooked, as socially differentiated needs and unequal access prevent all urban residents from benefitting equally from NbS in increasingly diverse urban societies[31,32]. The diverse social composition within and across cities, alongside environmental and technological factors, has been found to moderate exposure to and the accessibility and perceived benefits of NbS[33]. Thus, climate risk management of urban heat using NbS is also a challenge for environmental and social justice.

Socially equitable climate risk management has a spatial component too[34]. Marginalized groups and low-income households are typically constrained in their housing choices. Constraints include limited financial resources. In addition, discrimination in the housing market based on race, class, gender, or ethnicity limits housing options[9,35]. As a result, those groups often face poor housing quality and a lack of green and blue infrastructure[36]. While evidence supports the conclusion that marginalized groups experience higher levels of urban heat, the overlap between urban heat islands and residential areas of marginalized groups is not uniform across cities[35]. Social housing policies (e.g. rent control and non-profit housing) may substantially reduce such spatial and social inequalities.

While cities have begun to focus on vulnerable communities and prioritize the implementation of NbS in high-risk neighborhoods[37], a growing body of literature suggests that the introduction of NbS has inadvertently led to green gentrification in some cities[38,39]. The risks of displacement for vulnerable groups associated with green gentrification have been found to be more pronounced in contexts where social protection measures and affordable housing policies have been largely dismantled[38].

Thus, the implementation of NbS may further exacerbate the increasing socio-spatial inequalities that have resulted from shifts towards market-oriented urban housing systems and the increasing income inequalities that characterize current economic conditions[40]. Urban policy makers therefore have a choice[41]: They may risk the exclusion and displacement of low-income and marginalized residents by allowing (housing) investors and developers to capture the financial gains following the implementation of NbS. Alternatively, they can strengthen instruments and policies that mitigate displacement, e.g., rent control, social housing, land banks, and participatory design.

Although some cities have begun to promote policy integration, at least in the design and prioritization of adaptation strategies[37], integrating social and climate adaptation policies which are usually pursued by separate departments of the city's administration, remains a persistent challenge[42–44]. Climate adaptation policies still often focus solely on the implementation of NbS without recognizing socio-economic and spatial trade-offs[45]. Social policies rarely integrate differential exposures to climate change with the impacts of adaptation policies on vulnerable groups[46]. This leads to the main question of this paper: how can we ensure socially equitable climate adaptation to urban heat when promoting NbS?

To answer this question, we propose an integrated decision-making framework. The proposed decision-making framework is based on three sequential stages that are necessary to achieve socially equitable climate risk management: 1) climate risk assessment, 2) adaptation analysis, and 3) impact analysis (Fig. 1). To demonstrate what can be achieved by applying the proposed three-step decision framework, we use the Austrian capital, Vienna, as a test case. From an urban sustainability perspective, it is worth focusing on Vienna, which faces considerable challenges from increasing urban heat while striving to maintain resilient governance and robust social welfare policies, including social housing.

Results

Risk assessment: integrating hazard, exposure and vulnerability

Historic trend analysis reveals that hot days (HD), as an indicator of heat-related hazard, have been the primary driver of climate change-related risk over the least 50 years (Fig. 2, top box). Vienna experienced an increase in average annual air temperature of 1.8 °C since pre-industrial times, double the global increase over this period[47]. The pace of temperature rise has accelerated significantly in recent years and heat extremes are becoming more pronounced (see Table 1). The comparison between the climatic periods 1961–1990 and 1991–2020 shows an increase of 100% in the annual mean of HD. Very hot days (VHD) and Tropical Nights (TN), which were previously neglectable, now occur more regularly.

Data Source: Geosphere Austria. Exposure is also an important component of the risk of urban heat. Vienna's population has grown since the 1990s by about 500,000 people, reaching 2 million in 2024, amplifying exposure to hazardous heat events. However, the increases in hazard and exposure have been mitigated by a decrease in vulnerability. Populations in vulnerable groups, e.g., those with very low education and low income have declined in recent years (blue and green lines, Fig. 2, top box). Additionally, the share of heat-sensitive population groups, particularly those aged 85 and older, only marginally increased in the last decades.

Turning from historic to future trends of heat risk, our trend exploration (Fig. 2, top box) and the two RCP-SSP scenarios (Fig. 2, middle and bottom boxes) show that it is of utmost importance to consider the different heat-risk components in the formulation of adaptation strategies. The trend extrapolation indicates that HD will increase the most in the 2020-2050 time period. In addition, increased population implies higher levels of exposure, while demographic change is expected to result in a slight increase of the proportion of sensitive individuals aged 85 and older. If social policies continue to prevent high levels of low income and low education, as depicted in Fig. 2, top box, then adaptation strategies can prioritize limiting climate hazards, for instance through green and blue infrastructure.

Consideration of the two SSP-RCPs scenarios suggests a different prioritization of socially equitable climate risk management of urban heat. The SSP2-4.5 scenario suggests that the need for adaptation is strongly driven by demographic change, especially as the proportion of people aged 85 or older is foreseen to increase substantially. Expected expenditure for social policies and climate change mitigation measures assumed in this scenario minimize the other social vulnerabilities, such as low income and education levels. This set of risk factors differs crucially from the trend extrapolation, demanding prioritizing adaptation strategies to improve the situation of the elderly.

The worst-case SSP3-8.5 scenario requires adaptation strategies to tackle several critical developments. In addition to counteracting expected increased occurrences of heat hazards, strategies need to consider increased social vulnerabilities related to older and low-income residents. This poses a considerable, and highly complex challenge. Adaptation strategies should not only prioritize and finance the large-scale implementation of NbS in public spaces, but also need to focus on reducing high levels of poverty and supporting the elderly.

However, heat risk is unequally distributed over the Vienna cityscape (see Fig. 3). Utilizing Principal Component Analysis, we computed a composite Neighborhood Heat Risk Index (NHRI) to assess changing spatial patterns of risk (See Methods, A1: Spatio-temporal risk analysis). The NHRI is highest where moderate hazard (heat) intersects with high social vulnerability. The two principal components, PC1 - Socio-Economic Status (SES) and PC2 - Heat and Exposure, represent two contrasting features forming the spatial patterns of heat risk (see Supplementary Fig. 1). Heat hazard and exposure are most concentrated in the central parts of the city mainly due to sealed areas, few green spaces and high population density. Furthermore, high levels of vulnerable groups are concentrated in western and southern areas around the most central inner-city area and in the north and northeast

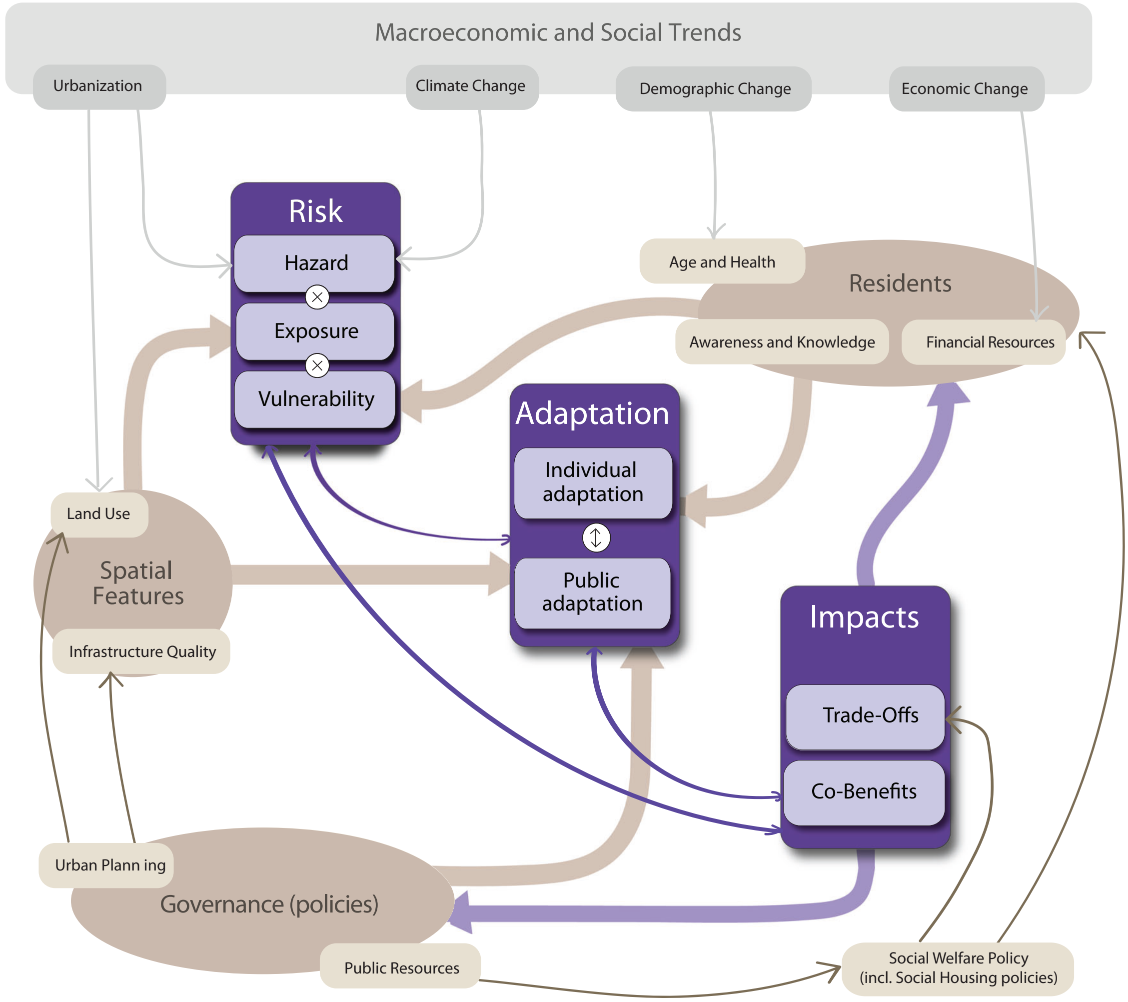

Fig. 1 | Three-step decision-making framework for socially equitable climate risk management of urban heat. The decision-making framework consists of three analytical steps (purple boxes): risk assessment, adaptation, and impact analysis. Purple arrows indicate how these steps are interconnected. Macroeconomic and social trends (gray boxes and arrows) serve as overarching influence factors shaping each analytical step, while urban-level governance, spatial features, and social structures (depicted as brown boxes and brown arrows) mediate these effects. Designed to be applicable to cities around the world, the framework illustrates how climate change adaptation and social policies can be integrated to achieve socially equitable urban heat risk management. It provides a comprehensive approach to prioritizing future climate adaptation while promoting environmental and social justice. The first step, risk assessment, integrates spatial and temporal trends in hazard, exposure and vulnerability factors. Climate change is the primary driver of hazard, whereas urbanization patterns contribute to hazard and exposure through land use. Socioeconomic factors, influenced by demographic and economic trends and mediated by public welfare policies, are key determinants of vulnerability. The risk assessment aims to: a) assess the (changing) relevance and interdependence of the risk factors – hazard, exposure and vulnerability; and b) provide a knowledge base for spatial, risk-based prioritization in the implementation of NbS. The second step, adaptation analysis, aims to supplement the knowledge by adding information on a) individual adaptive capacities based on factors such as age, health, financial resources, awareness and knowledge. The analysis aims to identify limits to individual adaptations, particularly for vulnerable groups, and provides crucial contextual information to inform the scope of public adaptation measures through NbS. Additionally, the adaptation analysis evaluates b) the cooling potentials and scalability of various types of NbS in public (and private) spaces in relation to existing spatial characteristics. It also assesses resident acceptance of NbS to ensure the legitimacy and effectiveness of adaptation strategies. The third step, impact analysis, examines trade-offs and co-benefits. A key focus is whether green gentrification poses a risk of displacement of vulnerable groups. This step looks at the effectiveness of existing policy instruments and identifies the need for additional governance mechanisms and housing policies, such as the provision of affordable housing or rent control.

of the city. The concentration of census tracts with high social vulnerabilities in the western and southern parts remains mostly consistent over four decades, while those in the north-east are declining. As a result, neighborhood-based heat risks have only decreased slightly. In quantitative terms, census tracts classified as being characterized by high and very high risks declined from 33% to 31%.

Adaptation strategies: private and public options

Urban heat is perceived as a problem from which citizens suffer more and more as evidenced by a representative survey conducted in 2022 (see Methods, D4: Survey Data). We found that 58% of respondents viewed urban heat as a problem. Outdoor thermal discomfort (63%) and poorer sleep quality is experienced during heat periods (62%). Moreover, 84% expect summer temperatures to be a more substantial burden in the future.

People utilize various measures to improve their indoor thermal comfort. Indoor temperature can be managed by ventilating at night and using window shading during the day. These measures are available to most citizens. More technical and costly solutions, such as installing air conditioning (AC) or external blinds, are not available to all households. In Vienna, only 7% of households have AC in all rooms; 28% have AC in some rooms of their dwelling. Thus, the majority of Viennese citizens relies on passive measures to manage indoor temperatures. However, this is often inadequate: 49% of all respondents (regardless of whether they have AC or not) report that after a spell of

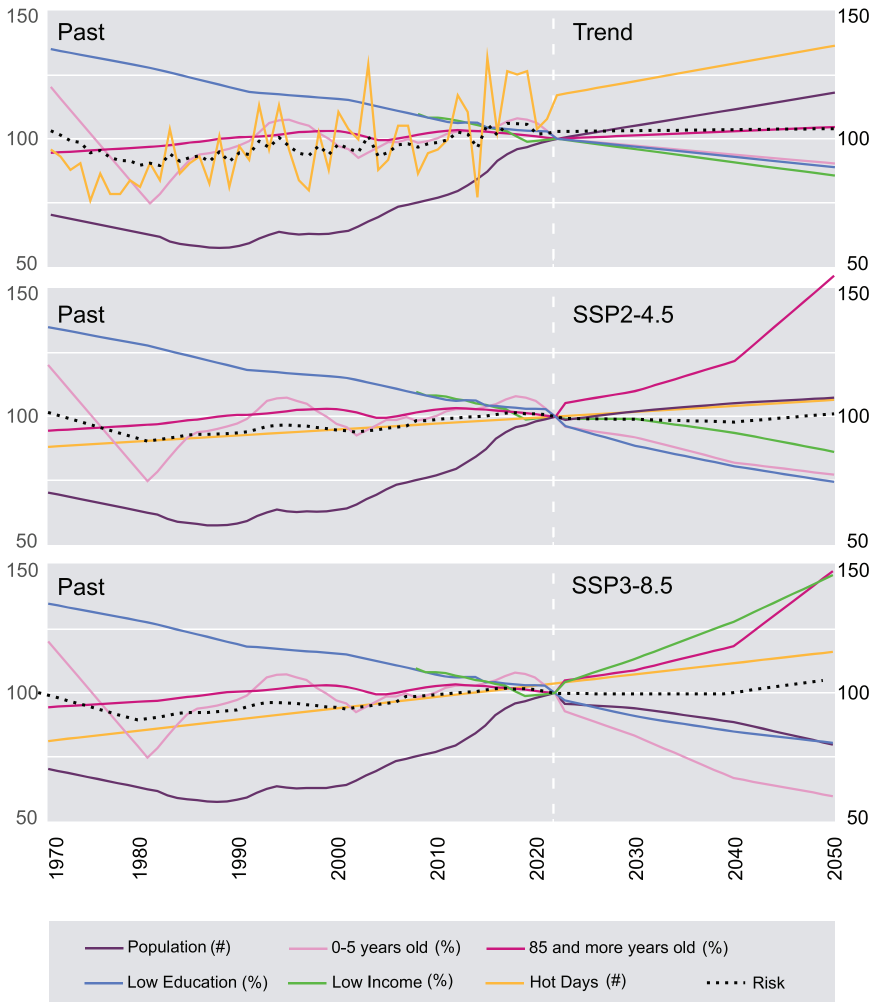

Fig. 2 | Indicators of hazard, exposure and risk: historical and projected. Figure 2 presents climate and socio-economic indicators with a common metric providing the basis for integrating climate and social policy. The common metric is established using a spatio-temporal normalization method (see Methods, A1: Spatio-temporal risk analysis). The values of each indicator are normalized across all scenarios and all time points to the reference year of 2022 (=100). The dotted risk line represents the arithmetic mean of all indicators. The historic socio-economic and population data, used in the left half of all three boxes, are census and register data from national providers (see Methods, D2: Population Data). In the top box, the historic annual number of hot days is based on measurement data. The 2020–2050 risk assessment (right side of the top box) extrapolates the measured numbers of HD as well as the socio-economic and population data. The two bottom boxes present two Socio-Economic Pathways – Representative Concentration Pathway (SSP-RCP) scenarios: SSP2-4.5 and SSP3-8.5. These scenarios were chosen to capture contrasting socio-economic and climate trajectories with direct implications for Vienna. SSP2 reflects moderate economic growth, gradual transitions to renewable energy, and sustained investments in education and social welfare making it well aligned with Vienna's existing economic and political stability. Due to Vienna's gradual renewable energy transition and historical warming trends, we paired SSP2 with RCP4.5 to more accurately reflect current trends rather than relying on the optimistic assumptions RCP2.6. In contrast, SSP3 reflects a fragmented and inward-focused geopolitical landscape, characterized by limited global trade that constrains technological transition towards renewable energies and aggravates inequalities and poverty levels. Pairing SSP3 with RCP8.5 reflects a stalled transition to renewables, aligning with the severe challenges Vienna could face under global instability and intensified warming trends. In summary, the SSP2-4.5 scenario presents moderate challenges, whereas the SSP3-8.5 scenario poses significant challenges for mitigation and adaptation (see Methods, A1: Spatio-temporal risk analysis for details). Historical and future HDs for the RCPs are chosen from the ÖKS15 time series (see Methods, D1: Climate Data) and future socio-economic pathways were calculated using national SSP change rates from the IIASA database attuned to local historical trends (see Methods, D2: Population Data).

several hot days their home is so hot that they have no way of cooling it down to a comfortable temperature. For 43% of all citizens, their living rooms are too warm on hot days, no matter what they do.

In addition to indoor options, urban heat can be addressed in public spaces. Viennese citizens make use of the city's public spaces: 40% avoid unshaded streets during the hottest hours of the day, and 30% increase their use of green spaces to seek relief from the heat. These findings highlight the importance of providing public spaces that are adapted to high and rising summer temperatures. In this regard, NbS in public urban spaces represent an important group of adaptation measures to compensate for limits to individual adaptation.

To estimate the cooling potential of public adaptation measures as realistically and feasibly as possible, a high-density implementation of commonly used NbS was modeled for a representative neighborhood (see Methods, Section A3: Assessing the potential of public adaptation). This level of NbS was then applied to all densely built-up areas in Vienna, which are the ones most vulnerable to urban heat. The effects of implementing NbS were then assessed by city-scale climate simulations. Compared to the city-wide status quo, the simulations with NbS measures implemented show that NbS can lead to a city-wide cooling effect of maximum -0.7 °C for the daily mean air temperature under clear-sky hot day conditions (see Table 2). The highest maximum daily air temperature difference, up to −1.4 °C, are found

Table 1 | Temporal development of the spatial average of climate indices in Vienna based on observational data

Climate indicator (days per year)	1961–1990	1971–2000	1981–2010	1991–2020
Summer Days (SU)	52.0	56.0	62.0	71.0
Hot Days (HD)	9.2	11.0	15.0	20.0
Very Hot Days (VHD)	0.0	0.3	0.6	1.5
Tropical Nights (TN)	1.1	2.0	3.2	5.2

SU: maximum daily temperature ≥25 °C; includes also HD and VHD.
HD: maximum daily temperature ≥30 °C.
VHD: maximum daily temperature ≥35 °C.
TN: minimum daily temperature ≥20 °C; as TN refer to the minimum daily temperature it indicates cooling during the night.

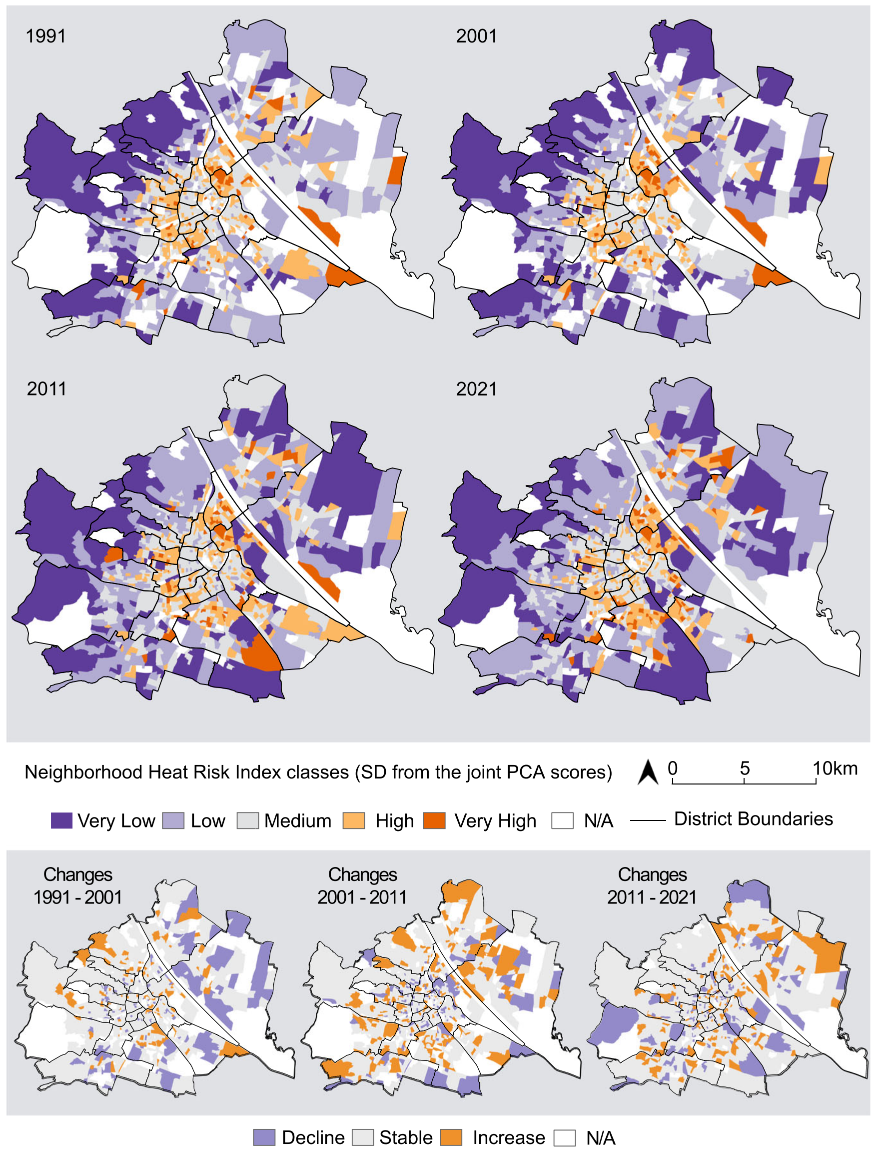

Fig. 3 | Vienna's changing neighborhood heat risk classes. The figures display Neighborhood Heat Risk maps at the top and Change maps at the bottom. The risk classes in the top maps are derived from the standard deviations of joint Principal Component Analysis (PCA) scores (see Methodology, A1), allowing for visualization of temporal dynamics. Results are shown for 1991, 2001, 2011 and 2021. The Heat Risk classes are defined as follows: Very Low Risk: < −1.5 SD; Low Risk: −1.5 to −0.5 SD; Moderate Risk: −0.5 to 0.5 SD; High risk: 0.5 to 1.5 SD; Very High Risk: > 1.5 SD. Changes between decades are calculated based on differences between the summarized and z-standardized Risk scores of the respective years. The Change classes are categorized as follows: Decline: < −0.5 SD change; Stable −0.5 to 0.5 SD change; Increase: > 0.5 SD change. Spatio-temporal integration and aggregation of the hazard, exposure and social vulnerability characteristics per census tract by means of PCA allows identification of the differential urban heat risk level of neighborhoods. The explained variance of around 70%, as well as the percentage of the components contributing to this variance, remain stable over the last three decades. According to decadal PCAs since 1991, the main components consistently contributing to the risk of neighborhoods are: PC1—Socio-Economic Status (SES) composed of education and unemployment levels (24.9–26.3% variance explained depending on the year); PC2—Heat and Exposure composed of heat extremes, population density and the inverse of the average tree canopy diameter (20.5–21.7%). Less important components of neighborhood heat risk are PC3—Age (12.3–14.4%) and PC4—Household Size (10.9% - 12.9%).

in some locations of the densely built-up areas where NbS measures were implemented in the model. Increasing the tree cover area from 9.1 ha to 207.1 ha in the densely built areas provides the highest contribution to the cooling effect ($\Delta T_{max} = -1.2$ °C). Increasing the number of green roofs in densely built-up areas from 0 to 5%, the Viennese average, has a negligible effect on the daily maximum air temperature ($\Delta T_{max} = -0.1$ °C).

Using climatological data and a combination of model simulations (see Methods, A3: Assessing the Potential of Public Adaptation), the cooling effects can also be evaluated in terms of specific climate indices, such as SU or HD. For the most recent climate period (1991–2020) the status-quo (SQ) simulation for densely-built areas shows an average of 78.3 SU, and 24.1 HD. The modeled NbS measures achieve maximum local decreases of 15 SU and about 13 HD and a spatially averaged decrease of 3.9 SU and 3 HD in the densely-built environment. These effects are comparable to the change in heat indices observed in Vienna between the period 1971–2000 and 1991–2020 (see Supplementary Table 1). The analysis shows that the local

Table 2 | Selected city-scale climate model results for densely built-up areas in Vienna

	T_{mean} (°C)	T_{max} (°C)	SU	HD
Status Quo (SQ, for climate period 1991–2020)				
Spatial average	26.7	30.3	78.3	24.1
Hottest location maximum	27.8	32.3	95.0	37.4
Current NbS Scenario compared to SQ				
Δ_{ave}	−0.2	−0.3	−3.9	−3.0
Δ_{max}	−0.7	−1.4	−15.0	−13.1
Future NbS Scenario under RCP4.5compared to SQ				
Δ_{ave}	–	–	−10.3	−6.7
Δ_{max}	–	–	−21.3	−17.2
Future NbS Scenario under RCP8.5 compared to SQ				
Δ_{ave}	–	–	−9.2	−6.5
Δ_{max}	–	–	−20.4	−17.0

The first two rows represent the Status Quo (SQ). For the climate period 1991-2020, the spatial average and the hottest location maximum for mean (T_{mean}) and maximum (T_{max}) air temperature, as well as average annual summer days (**SU**, $T_{max} \geq 25$ **°C**) and hot days (**HD**, $T_{max} \geq 30$ **°C**) are listed. The following rows show possible reduction in air temperature and climate indices for the dense-built-up areas where NbS measures are applied. Average (Δ_{ave}) and maximum (Δ_{max}) differences of the NbS simulations for current (1991–2020) and future climate (2021–2050) under RCP4.5 and RCP8.5 scenario are given. Data Source: Geosphere Austria.

maximum reductions of urban heat would be sufficient to compensate for the expected climate warming up to the middle of the 21st century and in case of an intermediate climate scenario (RCP4.5) for a longer term.

Looking at future climate conditions projected under RCP4.5, on average NbS measures could decrease SU by 10.3 and HD by 6.7 from 2021 to 2050 compared to the period from 1991 to 2020. Similarly, under scenario RCP8.5, reductions of 9.2 SU and 6.5 HD were modeled. Within RCP8.5, the anticipated urban heat increases of +22.9 SU and +15.8 HD for the time period 2071-2100 could be mitigated to average levels of +19.5 SU and +12.8 HD. Some areas may experience even greater cooling effects, with local increases as minor as +8.3 SU and +2.1 HD.

Vienna's citizens demonstrate considerable support for urban greening measures, as revealed by a choice experiment (CE) assessing their preferences and stated willingness to pay (WTP) for increased greenery in the city. A mixed logit model with correlated random parameters was used to simulate marginal WTP values for attributes of the proposed greening scenarios (see Supplementary Table 2). Remarkably, fewer than one-fifth of respondents favored the status quo when given the choice between maintaining the current level of greening or adopting one of two citywide NbS scenarios to be implemented over the next five years.

The CE scenarios included streetscape greening, defined as planting street trees and creating flower beds, and greening on buildings, encompassing the installation of green roofs and green facades. These measures were selected for their space efficiency, feasibility across most urban areas, dependence on investments, and widely recognized benefits. Further, to isolate preferences for urban greening from preferences for public space redesign, an attribute on street furniture, such as benches and fountains, was also included in the CE. (For an example of a choice card see Methods, A2: Assessing the limits to adaptation).

CE results indicate a clear preference for streetscape greening over interventions on buildings. Considering an increase in the prevalence of green elements from rare to everywhere, citizens were on average willing to pay €3.54 per year for trees and flower beds and €1.98 per year for greening of buildings (Supplementary Table 2). The highest WTP of almost €10 per year was associated with the alternative-specific constant (ASC) representing a preference for a change, independent of the greening attributes. The ASC most likely reflects intrinsic utility for participating in a greening program, but may also include unobserved attributes or underlying effects such as first-alternative bias. It may also, to some degree, stem from status quo or hypothetical bias – common issues in stated preference research. Therefore, any conclusions regarding the absolute ASC value should be made with caution.

Nevertheless, the findings highlight a general willingness among Viennese citizens to contribute financially to NbS. Based on the marginal WTP values, the mean combined WTP for a moderate NbS scenario, featuring all attributes increased from rare to frequent, is €14.27 per year. Aggregating these individual values for Vienna's population of 2.005 million inhabitants (2024) results in an annual societal WTP of almost €29 million. These results underscore the public's prioritization of accessible and visible green elements within the urban landscape.

Impact analysis: effectiveness of strategies to minimize inequalities

The paper uses the risk of gentrification and the role of green surroundings in housing choices as indicators of whether NbS are likely to contribute to socio-spatial inequalities. The risk of gentrification is examined through the use of an index distinguishing between two types of areas: areas that have experienced gentrification and areas that are at risk of gentrification. Areas are classified as gentrified if, in comparison to the citywide trend, there is an above-average decline in the number of socio-economically marginalized people, accompanied by an above-average increase in the number of socio-economically better-off households. In addition, there must be an above-average increase in market-based housing, e.g., unregulated private rental units and apartment ownership units. An area is considered to be at risk of gentrification if it meets at least one of the above criteria (see Methods, A4: Assessing socio-spatial inequalities: Gentrification Trends). Areas classified as gentrified or at risk of gentrification account for 18.4% (1991-2001), 14.4% (2001-2011) and 15.0% (2011-2021) of Vienna's residential areas.

A hierarchical logistic regression analysis with the binary gentrification index as the dependent variable was conducted to assess the factors influencing gentrification in three historical periods. Socio-economic factors, characteristics of the built environment, and the impact of Vienna's housing policies on gentrification were examined. Regarding socio-economic factors, the results indicate that, with a few exceptions, the presence of various vulnerable groups only marginally contributes to explaining a higher likelihood of gentrification in the subsequent period (see Supplementary Table 3). One of the exceptions is the presence of socio-economically marginalized people with third-country citizenship in 2001. This factor seemed to enhance the odds of gentrification in the following period. Between 2011 and 2021, population increase was a significant driver of gentrification.

As to characteristics of the built environment, distance to the city center only increases the likelihood of gentrification to a negligible extent. This is likely related to the fact that both inner-city and peripheral areas experience similar risks of gentrification (see orange areas in Fig. 4 for the 2001-2011 and 2011-2021 decades). However, construction of new dwellings within tracts significantly increases the odds of gentrification throughout all periods. This result is most likely explained by the construction of private market housing in these tracts. Risks of gentrification after 2010 are particularly associated with newly-built developments at the outskirts (see Fig. 4). Additionally, the odds of tracts to gentrify after 2010 were lower in areas that already had high levels of ownership of single-family houses and private market apartments (Supplementary Table 3).

Vienna's housing policies have resulted in several types of subsidized (social) housing units. Vienna started building municipal housing in 1925 and now maintains 220,000 units. Units built by limited-profit housing associations (LPHA) are the second important segment of social housing in Vienna. Since the 1990s, units built by LPHA have become the predominant type of social housing produced. Both municipal and LPHA housing units are strictly rent-controlled, and access is contingent upon meeting eligibility criteria. Private rental units in buildings that were constructed before 1945 are also subject to rent control (see Methods, D5 Dwelling Stock Data).

The regression analysis described above demonstrated that social housing has a mitigating effect on the likelihood of gentrification. In the

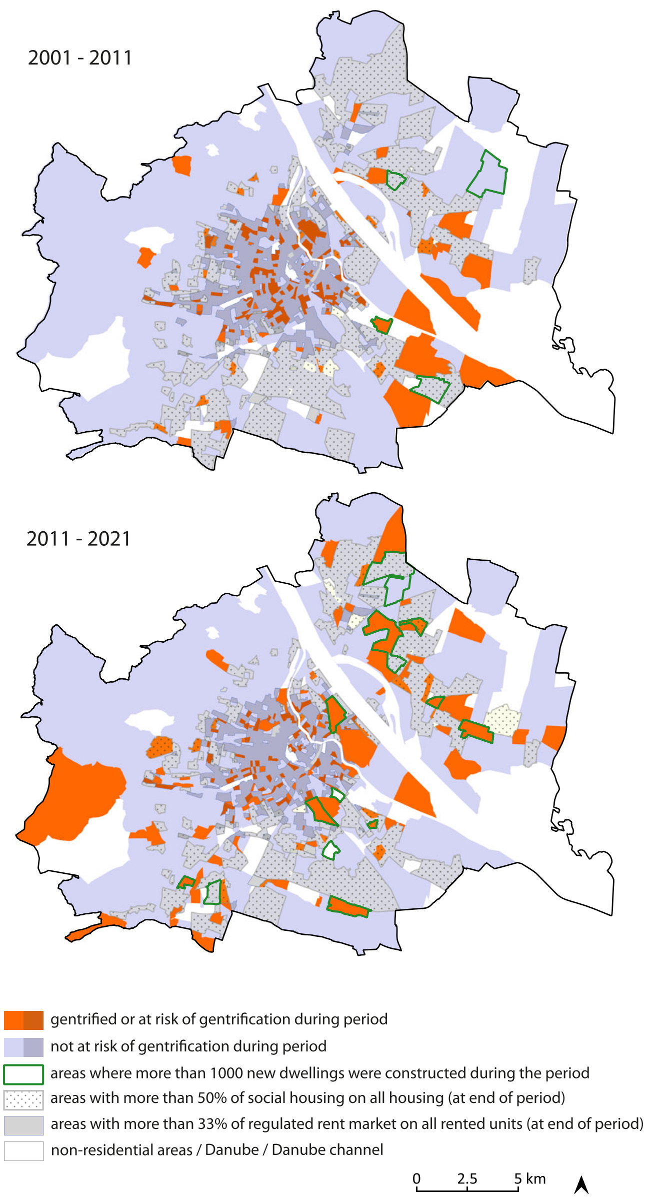

Fig. 4 | Gentrification trends in Vienna. Figure 4 illustrates gentrification tendencies in Vienna including its main factors over two different time periods: 2001–2011 and 2011–2021. Orange represents areas that were gentrified or at risk of gentrification during the period, light purple indicates areas not at risk of gentrification. Using logistic regression, the main factors influencing gentrification tendencies were identified (see Methods, A4: Assessing socio-spatial inequalities: Gentrification Trends). Main influencing factors include areas where more than 1000 new dwellings were constructed during the period, areas with more than 50% of social housing in all housing and areas with more than 33% of regulated rent market on all rented units at the end of the period.

1990s, neighborhoods with high levels of municipal housing were less likely to gentrify. During the 2000s, however, areas with a high proportion of rent-regulated private apartments, which predominate Vienna's city center, had an increased likelihood of gentrification (see Fig. 4). This is likely due to two facts. First, the effectiveness of rent control in the regulated private rental market was weakened by reforms in the 1990s. Second, the proportion of social housing in central Vienna is insufficient to mitigate gentrification. For the 2011-2021 decade, the regressions demonstrate that a 1% higher share of municipal or LPHA housing significantly decreases the likelihood of gentrification by 4 to 5%. Consequently, policies that facilitate the construction and preservation of municipal housing, as well as requirements that a proportion of apartments in new developments must be subsidized social housing, serve and have served to mitigate or even prevent gentrification.

While social housing in Vienna mitigates gentrification generally, green residential surroundings have weak and mostly statistically insignificant effects on the choice of the place of living. Based on the representative survey, (see Methods, D4: Survey Data), data at the household-level indicate that residential choices in Vienna are largely unaffected by the amount of urban green. This is the case both retrospectively regarding the choice of the current residential location and prospectively for an envisaged future residence. In retrospect, households chose a greener area for their current residence if they had been content with the greenness of their previous neighborhood. However, the low total explained variance in the greenness of the current residential location indicates that green residential choice is dominated by other drivers of residential choice: as income, age, level of education, migratory background, or biographical events (see Supplementary Table 4).

Similarly, on the household level, the intention to change residence is not associated with the discrepancy between the greenness of the current neighborhood and the greenness of an envisaged future residence. Younger households, renters, the less affluent and those living in units that are older, over-crowded or without a garden or balcony, show a stronger intention to move than other households. However, adding the desire for better access to green or blue areas does not yield additional explanatory power (see Supplementary Table 5). Unsurprisingly, residential mobility is most strongly tied to individual capacities and insufficient housing conditions.

Thus, survey data support the conclusion that green gentrification, in the sense of a deliberate choice of a green location by people moving within the city, is only marginally applicable to Vienna, at least under current circumstances. As a result of this and its strong housing policies, in Vienna, possibly in contrast to many other urban areas, NbS can be implemented without a significant risk of increasing socio-spatial inequalities.

Discussion

Our study presents a structured way to overcome the current policy fragmentation of climate adaptation and social policies. The integration of current policy silos is accomplished through an innovative, three-step decision-making framework that forms bridges between adaptation options, such as NbS, and social and spatial equity issues. The decision model integrates climate data, socio-economic data and spatial analysis. By applying the framework to the Viennese context, we demonstrate the value of using an integrative framework to guide implementation of adaptation measures. This framework provides the foundations of a socially equitable adaptation program, particularly one that avoids the risk of green gentrification. The framework also helps to formulate context-specific policy strategies by examining a range of socio-economic factors relevant to urban heat adaptation, such as age and income. So, what do our findings mean for designing a socially equitable and effective climate risk management in the urban context through overcoming policy siloes?

For Vienna, our long-term historical risk assessment allows us to isolate the increasing heat hazard from increasing exposure. In addition to the increase in heat extremes, population growth has been the second major driver of increased climate change risk in Vienna in recent decades. In contrast to existing studies that focus primarily on the effects of hazard and exposure[8], our results highlight the importance of recognizing trends in social vulnerability levels. In past decades, social vulnerability levels in Vienna declined. The main reason for this trend were economic and social policies which increased income levels for low-income households and also improved educational levels, while the share of health-sensitive groups, such as the elderly, remained stable. Looking into the future, however, strong growth in population over 85 will be a major factor in increased risk. Thus, new social policies will be needed to address this dimension of social vulnerability.

The implications of population characteristics for socially equitable climate risk management should not be underestimated. In urban contexts, where the number of people in socially vulnerable groups may be rising, climate change adaptation policies will increasingly need to integrate social policies, such as income support, housing, health and education policies. For urban contexts where these social welfare policies are in place, such as Vienna, the results of our near-future risk assessment show that these social welfare policies need not only to be maintained but augmented by policies with priorities depending on expected future developments. For example, policies will need to target older residents due to demographic shifts in Vienna.

The strategy for socially equitable climate risk management investigated in this paper is to improve the living conditions of vulnerable groups. Options reviewed include cooling of interiors, green roofs or facades, and NbS in public spaces. Consistent with other research indicating that cooling homes is a particular challenge for vulnerable groups[15,16], we found evidence through our household survey that adaptation options available to individual households are limited. Although the survey did not focus exclusively on vulnerable groups, it showed that the effective cooling of homes requires rather costly solutions, which often have to be approved by the landlord. This is particularly relevant in the Viennese context, where the majority of residents are tenants, which is even more the case for vulnerable groups. While this situation may be very different in other urban areas, the financial limits of low-income households would still be a major constraint. As the City of Vienna provides homes for 220,000 households, the role of the city as a landlord may complement urban heat adaptation policies: the greening of public spaces, facades and roofs, thermal insulation and shading in the City's residential buildings are important adaptation polices on their own.

Importantly, a socially equitable climate risk management strategy that focuses exclusively on cooling individual homes may not be the most feasible, desired, or effective approach. At least for Vienna, as evidenced by the results of the conducted choice experiment, there is a willingness to pay for implementing NbS. NbS measures in streetscapes and public spaces are preferred over NbS measures on roofs and facades. Moreover, the results of the climate modeling indicate that the implementation of NbS in public space is the most effective approach to managing the risks of climate change. While the concrete effects depend on the specific urban structures, the addition of trees has the greatest impact on cooling at the street level whereas green roofs have a minimal effect on daily maximum air temperature. Due to advection of cool air, NbS in public spaces has the potential to reduce Vienna's air temperature sufficiently to offset anticipated climate warming up to the middle of the 21st century.

Given the preference for, and effectiveness of, NbS in the streetscape and public space, the design of a socially equitable risk management strategy for Vienna must consider issues of spatial justice. Ideally, this would prioritize greening NbS in neighborhoods where disproportionally higher heat loads, exposure and social vulnerability intersect. However, the results of our spatio-temporal risk analysis have shown that high heat exposure does not necessarily overlap with the spatial distribution of higher vulnerability levels. Our results confirm a more general pattern in which the overlap between the distribution of urban heat islands and vulnerable groups varies across cities worldwide[35].

Previous research has shown that vulnerable groups tend to face a high risk of displacement after the implementation of NbS[38], especially when implemented in high-risk neighborhoods. Our results indicate that Vienna's current low gentrification risk is the dividend of a century-long social housing policy which largely mitigates the risk of displacement for vulnerable groups. Vulnerable groups that live in areas dominated by social housing are not exposed to risks of displacement. However, vulnerable groups that live in areas dominated by the weakened rent-regulated, pre-war housing segment are exposed to higher risks of displacement. It is critical to acknowledge that these areas could potentially experience future green gentrification, particularly given the rising need for NbS implementation and the increasing willingness to pay for such benefits. Nevertheless, Vienna's example provides evidence to recent comments on the importance of anti-displacement tools and policies accompanying the implementation of NbS[41].

Abstracting from the case of Vienna, it seems that urban NbS can be implemented without increasing socio-spatial inequalities, but only if strong social housing policies are in place. Furthermore, socio-demographic and economic factors, such as age, income, education level and biographical events, are the dominant influences in housing choices. In Vienna, green spaces currently do not provide additional pressure on already weak gentrification dynamics. While our analysis did not find a strong historical correlation between greening and gentrification, we recognize that future dynamics may differ, driven by escalating heat stress, the scale of greening efforts, changing housing market conditions, or the presence of alternative adaptation measures. In cities with less effective social housing policy and a weaker welfare system, the proposed impact analysis could be expected to evidence a more pronounced impact of additional green spaces on the housing market. Consequently, such cities are in a less favorable position for rolling out socially equitable NbS in public spaces and should adopt innovative, context-sensitive social housing policies to mitigate these risks.

Overall, our study highlights the context-specific underpinnings of the spatial and temporal interactions of hazard, exposure and vulnerability. Consideration of the underlying factors are critical for designing integrated, robust policy approaches at the local level. Assessing the relevant factors is only possible through a multidisciplinary assessment which combines climate, socio-demographic and spatial data, as our application to the Vienna test case shows. In sum, to design effective and socially equitable policies and avoid unintended trade-offs our study highlights the importance of overcoming current policy silos in cities' approaches to urban heat adaptation.

Methods

This section first presents all relevant data sources that feed into the analytical steps. We have structured the data sources from D1 to D5. The analytical steps from A1 to A5 follow.

D1: Climate data

Measurement data of historic climate indices are obtained from data.wien.gv.at[48]. Data underlying the long-term historical and future scenarios of heat risk are chosen from the ÖKS15 time series for Vienna[49–51]. The time series encompasses the period from 1971 to 2100 and employs 13 bias-corrected EURO-CORDEX models.

The small-scaled simulations of the historic spatio-temporal risk analysis (Fig. 3) and future urban climate for the City of Vienna were performed with the urban climate model MUKLIMO_3 (in German: 3D Mikroskaliges Urbanes KLImaMOdell) developed by the German Weather Service (DWD). The thermo-dynamical version of the model described in Sievers[52] with model updates released in 2020 was used. The model uses Reynolds-averaged Navier–Stokes (RANS) equations and includes parametrization of vegetation and building morphology based on terrain elevation, land use types and spatial distribution of land use parameters such as building density, building height and wall area index, sealing fraction and tree cover. The model domain covers the City of Vienna and its immediate surroundings with a grid size of 314 ×239 points and a horizontal grid spacing of 100 m. The vertical resolution of the 3D model with 39 levels varied from 10 to 100 m with higher resolution near the ground to a maximum height of about 1000 m. Previously, the model has also been used to investigate the impact of green and blue infrastructure, including green roofs, to mitigate the UHI effect. The model configuration used in this study is adapted from a recent multi-scale modeling approach[53]. The simulations were conducted for a chosen clear-sky hot day (19.07.2014) representative for heat conditions during a summer period in Vienna.

In combination with meteorological measurements and regional climate model scenarios from the EURO-CORDEX project[54] representative for the regional background climate, MUKLIMO_3 was used to derive climate indices (SU, HD, VHD, TN) related to heat conditions on urban scale[55,56]. The climate indices analyzed in this study are selected to comply with standardized indices (SU, TN) for Climate Change detection recommended by Expert Team on Climate Change Detection and Indices (ETCCDI)[57] and to include extreme events that have severe impact on thermal comfort and public health (HD, VHD). An ensemble of 8 model outputs (Global Climate Model/Regional Climate Model combination) was used to project future heat indices in Vienna until 2100 based on Representative Concentration Pathways (RCP)[58]. The RCP4.5 (intermediate) and RCP8.5 (worst-case) scenarios of the IPCC-AR5[59] were investigated to show a different climate development. It should be noted, that, based on analyzing historic trends of heat indices, current EURO_CORDEX models seem to underestimate the increase of extreme indices such as HD for Europe, hence also for Vienna[60].

D2: Population data

Socio-economic and socio-demographic data were obtained upon request from the Statistical Department of the City of Vienna and the Austrian Statistical Office. Data for the smallest available statistical unit (census tracts) were collected for the years 1991, 2001, 2011 and 2021. Proportions relative to the total population were calculated for educational attainment, citizenship, age groups, household size and household composition.

Long-term data ranging from 1971 to 2022 was obtained from STATcube—Statistical Database of Statistics Austria[61]. This long-term data was used to project selected indicators of social vulnerability (population under 5 and over 85, population with low education, and population with low income). First, a trend extrapolation used the historic annual average growth rates to project the selected indicators until 2050. Second, scenarios based on national change rates of the Shared Socio-economic Pathways (SSP) database by the IIASA[62–65] were developed. To account for regional variations of the national SSP change rates from the IIASA database two approaches were used. For population and age groups, z-scores of annual average growth rates based on regionalized population and age projections were calculated[66]. The z-score of Vienna was used to weight the national change rate of the different SSPs. As no such regionalized projections exist for income and education, we collected change rates for those indicators based on the Degree of Urbanization from the Eurostat Database[67,68]. The deviation of urban areas in from the national change rate was calculated and used for weighing the national change rates of the different SSPs.

D3: Green infrastructure data

Data from the municipal tree cadaster of public trees was obtained from the open database of the City of Vienna which omits trees on private land[69]. The municipal tree cadastre only allowed for a small-scale, long-time analysis of the development of green infrastructure from 1991 to 2021. Using GIS, we calculated a buffer of 250 m surrounding buildings in residential areas. We summed the number of trees and calculated mean tree top diameters for the years of 1991, 2001, 2011 and 2021. In a second step we calculated the average number of trees and tree diameters for all buildings within a census tract, resulting in a proxy indicator of public green infrastructure at the census tract level.

D4: Survey and CE data

Standardized online questionnaires which included the choice experiment (CE) were distributed in Vienna in two cross-sectional surveys in May and September of 2022. Already in May, the summer of 2022 featured frequent high daytime and night-time temperatures; thus, the issue of urban heat was presumably salient in the survey population.

A market research company contacted Viennese residents aged 18 to 69 years who had preregistered as panel participants. The samples of 1100 and 1081 residents were representative of the socio-demographic distribution in Vienna's population in terms of gender, level of education and city district, within the age span of 18 to 69 years (see Table 3). The questionnaire was pre-tested for clear language and comprehensibility with n = 100 respondents, whose responses were checked for implausible patterns that might point to design shortcomings or implementation errors. As no unusual data were detected, data collection continued unchanged for the remainder of the survey. All items were originally worded in German.

D5: Dwelling stock data

Data on the dwelling stock per census tracts for the years 1991, 2001, 2011 and 2021 were obtained upon request from the Statistical Department of the City of Vienna. Dwelling stock data was obtained to analyze changes in each segment of the housing stock supply within census tracts. Vienna's housing supply consists of the following segments: (a) private ownership of single-family homes, (b) private ownership of apartments, (c) free market apartment rental, (d) rent-controlled rentals, and (e) social housing. Social housing is further divided between municipal housing and limited-profit housing associations (LPHA), both of which are rent-controlled while access is contingent upon meeting different eligibility criteria[70].

Table 3 | Shows the sample structure and how it relates to the composition of Vienna's demography

Socio-demographic characteristics	Sample		Population of Vienna
	Absolute frequency	Relative frequency	Relative frequency
Gender			
Male	967	49%	48.8%[a]
Female	1.016	51%	51.2%[a]
Age			
<30 years	438	22%	34.1%[b]
>30 – 55 years	1.019	51%	36.9%[b]
>55 years	526	27%	29.0%[b]
Highest Education			
Elementary School, Apprenticeship	940	47%	53.3%[c]
Highschool	507	26%	21.5%[c]
Tertiary Education	536	27%	25.3%[c]
Monthly net household income			
<2.000€	579	35%	
2.000–4.000€	712	43%	
>4.000€	350	21%	

[a]City of Vienna. (2020).
[b]Statistics Austria.
[c]City of Vienna. (2018).

A1: Spatio-temporal risk analysis

To perform the spatio-temporal risk analysis, climate, population, and green infrastructure data were merged at the census tract levels. All indicators were normalized using the constrained min-max Adjusted Mazziotta-Pareto Index (AMPI) approach suggested by Mazziotta & Pareto[71]. The AMPI approach has the advantage that all values across all periods of time are normalized and have a common reference point, thus allowing for comparisons over time. The baseline value is set to 100. Development trends over time are shown by decreases (less than 100) and increases (more than 100). We used this approach for two assessments with different common references: a) the historical spatio-temporal risk assessment uses 1991 and b) the long-term risk assessment uses 2022 as reference year.

The AMPI value for the "constrained Min-Max method" was calculated accordingly:

$$y_{ij}^{t} = \frac{x_{ij}^{t} - x_{0j}}{Max_{xj}^{t4} - Min_{xj}^{t1:t4}} * 60 + 100 \quad (1)$$

Whereas: i = unit and j = indicator at time t (which refers to the years 1991, 2001, 2011, 2021), x_{0j} is the mean value of 1991 and

$$Max_{xj}^{t} = 100 + \left(\frac{(Max_{xj}^{t1:t4} - Min_{xj}^{t1:t4})}{2} \right) \quad (2)$$

$$Min_{xj}^{t} = 100 - \left(\frac{(Max_{xj}^{t1:t4} - Min_{xj}^{t1:t4})}{2} \right) \quad (3)$$

Figure 2 shows the results of applying the AMPI methodology to the long-term risk analysis. The 2020-2050 risk assessments are based on a trend extrapolation (Fig. 2, top box). The middle and bottom box projections of Fig. 2 are based on two Socio-Economic Pathway-Representative Concentration Pathway (SSP-RCP) scenarios. The two scenarios – SSP2-4.5 and SSP3-8.5 – not only envision differing challenges associated with climate change mitigation and adaptation, but also represent two contrasting climate change scenarios as well global geo-economic and political settings potentially affecting Vienna[72].

SSP2 offers a balanced scenario, reflecting moderate economic growth within a context of uneven global development[72], which aligns with Vienna's current economic and political stability. The gradual technological shifts towards renewable energies and sustained investments in education and social welfare envisioned in SSP2 align with Vienna's priorities and policy orientations. This scenario allows us to explore a future where Vienna achieves steady (economic and population) growth, adapting as much as feasible to global and local climate challenges while maintaining its socioeconomic foundations and commitment to sustainability and inclusivity. Given Vienna's current economic and political trajectory, along with its historic warming trends, we intentionally avoid using an overly optimistic scenario. Instead, we chose to pair SSP2 with RCP4.5, representing a more realistic climate pathway compared to the more ambitious RCP2.6.

SSP3 offers a contrasting scenario of a fragmented and inward-focused geopolitical landscape, a perspective that has become increasingly realistic in light of recent events such as the SARS-CoV-2 pandemic and the Russian-Ukrainian war. In this scenario Vienna would face challenges stemming from security-oriented policies, which would limit investments in education and social welfare alongside an envisioned economic downturn, fueling increased levels of poverty[64,72]. Additionally, the combination of low fertility rates, migration and urbanization would result in a markedly old age structure[72]. The fragmented geopolitical environment would also restrict global trade opportunities, slowing down technological transitions to renewable energies. This trade limitations are the primary reason SSP4 was not selected, as SSP4 envisions growing inequalities as well but also assumes rapid technological advancements in high-tech economies. Given the constraints on global trade and slow technological progress, SSP3 is paired with RCP8.5, reflecting the limited climate change mitigation efforts expected in such a scenario.

For the historic spatio-temporal risk analysis (Fig. 3), we performed a joint Principal Component Analysis (PCA). In doing so, we followed recent approaches that investigated spatio-temporal changes of social vulnerability[73,74]. Initially a set of 17 variables covering hazard, exposure and vulnerability were used in the PCA. First, we excluded variables used for the joint PCA by testing multicollinearity using the Kaiser-Mayer-Olkin (KMO) value of > 0.6, a significant Bartlett test, and avoiding communalities (< 0.5). Based on these pre-tests, three variables (Single Parents, Average Number of Trees and Share of people with vocational training) were excluded. This resulted in a final set of 14 variables (see Supplementary Table 6). Second, we conducted the principal component analysis (PCA) using the Varimax rotation extracting principal components (PCs) with Eigenvalues > 1. Rotated PCs and factor loadings (> I0.5I) were interpreted for coherence in terms of orthogonal factors that can be considered independent from each other. Third, single year PCAs (1991, 2001, 2011, 2021) were calculated to allow the analysis of changes in drivers for the respective years. Fourth, scores for the Neighbourhood Heat Risk Index (NHRI) were calculated by summing up the PC scores weighted by the percentage of variance explained of the respective PC. Fifth, the NHRI was classified into 5 classes using the joint PCA's standard deviations to show changes over time (see Fig. 3). Sixth, the factor loadings of the yearly PCAs with 4 classes were mapped (see Supplementary Fig. 1).

A2: Assessing the limits to adaptation

To assess citizens' preferences and willingness to pay (WTP) for NbS to reduce urban heat, a choice experiment (CE) was conducted as part of the representative survey (see Methods D4: Survey and CE Data). CEs are a well-established method to assess how respondents perceive hypothetical changes. Based on Lancaster's Characteristics of Value Theory[75], the change (valuation object) is described by a range of attributes with different levels, which vary between the choice tasks[76].

The CE consisted of two greening attributes, distinguishing between measures in streetscapes (trees and flowerbeds) and measures on buildings (green roofs and facades). The attributes relate to the most important groups of small-scale greening measures implemented in cities, which are widely known, dependent on financial resources, and within the sphere of influence of city governments. The selection of attributes and their respective levels were discussed in detail within the project team and with experts working for the City of Vienna. An additional street furniture attribute was included to allow for isolating preferences for urban greening from those for the redesign of public spaces. A cost attribute (varying from 1 to 6€/month) presented as a monthly earmarked fee to an urban greening fund was included to estimate WTP. Table 4 gives an overview of the attributes and defines how the levels were presented to the respondents.

One-third of the respondents were given an additional attribute (Attribute 4) highlighting the temperature change associated with the scenario, while another third received additional pictograms about the heat-reducing effect of urban greenery as part of Attribute 1 and 2. An analysis of the differences between the three operationalization approaches for representing cooling effects is part of ongoing research. However, in the present analysis the samples were jointly estimated. While minor alterations in attribute depiction may influence preferences to some extent, the base preferences are assumed to remain consistent across samples. Further, pooling the samples increases statistical power, leading to more robust and precise parameter estimates.

Using the software Ngene choice cards with a high D-efficiency as optimality criterium were compiled, resulting in two sets of 24 choice cards each. The five-attribute design was constrained to link higher levels of greening attributes to higher temperature reductions. Later, all final scenarios were checked for plausibility and the presence of dominant choices, and a pre-test was conducted with 100 respondents. Finally, each respondent was randomly assigned to either the four- or the five-attribute CE and presented with one of four blocks of choice cards, each consisting of six choice situations in a random order, in which they had to choose between two scenarios and the status quo (SQ) (see Fig. 5 for one example of a choice situation).

The CE responses were estimated using a Mixed Logit Model (MXL) with correlated random parameters. This model allows for preference heterogeneity, as the parameters are not considered fixed but are derived from a statistical distribution. This approach addresses the limitations of simpler multinomial logit models (MNL), such as the restrictive independence of irrelevant alternatives (IIA) and the requirement for independent and identically distributed error terms (IID). In our analysis the main attributes were treated as normally distributed, while the cost attribute as lognormally distributed.

Both MXL and MNL are based on McFadden's random utility framework[61] This framework states that the indirect utility (U) of each respondent (i), consists of

(1) a deterministic part (V), that is typically a function of observed attributes (X_{itj}) of the observed alternatives multiplied by their respective parameters (β_i), and

(2) the random error term (e_{itj}), which represents all influences on the decisions that are unobservable.

In a MXL the conditional probability that a specific alternative is chosen is described as

$$P_{ijt}(\beta_i) = \frac{exp(X_{itj}\beta_i)}{\sum_{k=1}^{K} exp(X_{itk}\beta_i)} \tag{4}$$

Table 4 | Explanation of the attributes and attribute levels used in the choice experiment

Attribute	Explanation of Attribute Levels (translation of the material presented to the respondents)
Attribute 1: **Measures on streets ('Streets')** Street trees, planters and green strips	rare
	• There are many streets without greening. There is a tree in front of some houses.
	scattered
	• The number of trees and plant troughs will be increased slightly. There is a tree in front of every fourth house.
	frequently
	• The number of trees and plant troughs is considerably increased. There is a tree in front of every second house.
	everywhere
	• The number of trees and plant troughs is increased significantly. There is a tree in front of almost every house.
Attribute 2: **Measures on building ('Build')** Green facades and roofs	rare
	• Green roofs and façades are a rarity.
	scattered
	• Every third building that is suitable for greening is greened.
	frequently
	• Every second building that is suitable for greening is greened.
	everywhere
	• Every building that is suitable for greening is greened.
	rare
	• There are a few benches and drinking fountains.
Attribute 3: **Street furniture ('Furniture')** Benches, drinking fountains and water sprinklers	scattered
	• Additional benches will be installed so that they can be reached within 5 minutes from every house. Drinking fountains are installed at a few selected locations.
	frequently
	• Additional benches are installed so that they can be reached in 3 minutes from every house. Drinking fountains and water sprinklers are installed in squares and in some streets.
	everywhere
	• Additional benches are installed so that they can be reached in 1 minute from every house. Many drinking fountains and water sprinklers and a few fountains will be installed.
Attribute 4: **Effect on urban heat ('Heat')** Cooling effect of the implemented measures	No cooling effect
	• It is very hot on summer days. The number of days with 30 °C or more is high and increases over the years.
	A slight cooling effect
	• The measures result in slight cooling in summer. (Average reduction of one degree Celsius in the surrounding area)
	A considerable cooling effect
	• The measures result in a noticeable cooling effect in summer. (Average reduction of two degrees in the surrounding area)
	A significant cooling effect
	• The measures result in a significant cooling effect in summer. (Average reduction of four degrees in the surrounding area)
Cost attribute: **Monthly fee ('Cost')** Individual contribution to earmarked greening fund	1€, 2€, 3€, 4€, 5€, 6€ per month

The unconditional choice probability, which assumes that the vector of parameters β_i follows the distribution $f(\beta_i|\Omega)$, is expressed as

$$P_{ijt}(\beta_i|\Omega) = \int_{\beta_i} \left[\frac{exp(X_{itj}\beta_i)}{\sum_{k=1}^{K} exp(X_{itk}\beta_i)} f(\beta_i|\Omega) \right] \mathrm{d}\beta_n \tag{5}$$

The unconditional choice probability can then be formulated as a log-likelihood function:

$$LL(\Omega) = \sum_{i=1}^{N} ln(P_{ijt}(\beta_i|\Omega)) \tag{6}$$

Since the integral for parameters described by statistical distributions is not computable with a simple log-likelihood maximization, a simulated log-likelihood maximization is applied. Specifically, this study utilizes 2000 Sobol draws[77] with Owen[78] and Faure-Tezuka[79] scrambling[80]. For the WTP simulations, we applied the Krinsky and Robb method[81], using 10,000 iterations and 100,000 draws per iteration from a multivariate normal distribution (with a vector of estimated parameters from the MXL model as mean and corresponding asymptotic variance-covariance matrix, an inverse Hessian, as the variance). This approach enabled us to calculate standard errors and confidence intervals of obtained welfare measures[82,83]. All econometric analyses were performed using MATLAB software with custom-written codes (link to codes, anonymized for review purposes).

A3: Assessing the potential of public adaptation

The state-of-the-art microclimate model ENVI-Met[84,85] is used to assess and quantify effects of technical and NbS on the local microclimate in a typical Viennese quarter. ENVI-Met is a three-dimensional model, representing

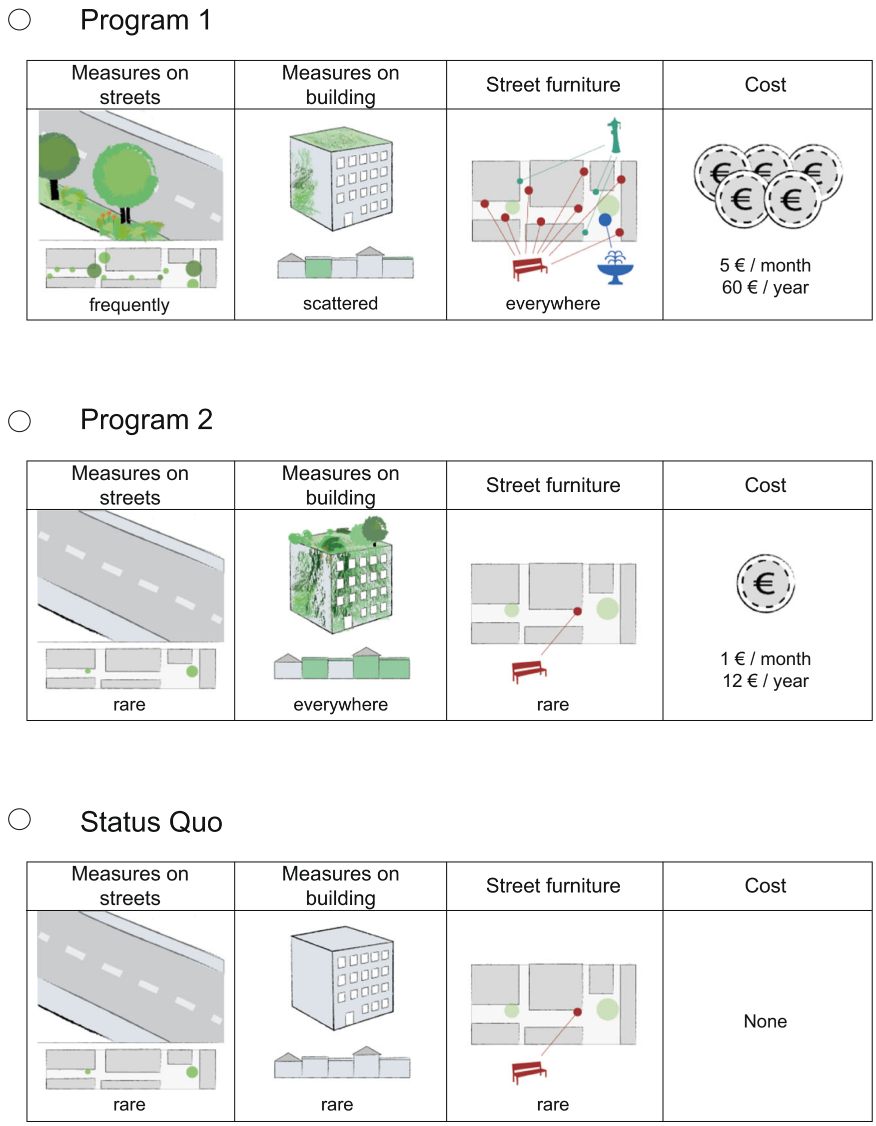

Fig. 5 | Example of a four-attribute choice card. SQ Status Quo.

atmospheric processes and interactions between buildings, surfaces, and plants using coupled atmospheric, soil and vegetation models at spatial scales from 0.5 to 10 meters.

The Viennese quarter "Supergrätzl", located in the 10th district of Vienna, was selected as the site for study. This area serves currently as a demonstration and urban experimental site following the principles of the internationally known "Superblocks" of Barcelona. The "Supergrätzl" is also representative of a common Viennese building pattern, an ensemble of urban building blocks stemming mainly from the pre-WWI era with high building density[53] and a high heat. This makes it an appropriate case study for demonstrating the potential of NbS in the densely built-up areas part of Vienna.

Four streets, shown in pink and dotted orange, form the boundaries of "Supergrätzl". Fifteen building blocks are formed by intersections of the two east-west streets and four north-south streets within this area. Each tile represents a typical Viennese building block with residential buildings except for the tile in the North-East corner where a public park is located. Starting with the status quo, bundles of NbS measures (e.g. trees, unsealed parking spaces etc.) were added separately in ENVI-Met to assess their specific cooling potential. In total, five different bundles of measures were applied (Fig. 6). All measures are situated within public space, except for the green roof and facades, which are implemented on buildings. For each of the bundles, its feasibility was considered prior to its model implementation. Feasibility preserved adequate areas for transport and parking, required distances between trees and technical requirements for sun sails. With respect to the grid resolution, an area of 2 ×2 m is the minimum area a given measure can comprise, i.e. an additional tree requires 4 m² of unsealed soil. The changes of area occupied by a given type of usage (e.g. building, streets, unsealed surface) for the *Supergrätzl* are depicted in Table 5.

Next, we evaluated the cooling effect of NbS and its effectiveness in counteracting the expected increase in urban heat due to climate change at the city scale. NbS measures were upscaled to all areas in Vienna with land use characteristics similar to those in "Supergrätzl". Urban climate simulations using the model described in section D1: Climate Data were then performed considering several climate scenarios. Climate indices based on simulations with NbS measures are compared with a reference simulation without any NbS adaptation measures for both current and future climate conditions (see Results, Adaptation strategies: private and public options).

The potential change of parameters in all densely built-up areas as well for the status quo in the city of Vienna as a whole are presented in Table 5. Compared to the average land use characteristics in Vienna, the densely built-up areas have a higher percentage of buildings and sealed surfaces and a lower amount of vegetation. In the simulation of the NbS scenario, the building density remains unchanged, while the sealed surfaces decrease and vegetation on roofs, streets and new park areas are implemented. The increase in the number of trees was implemented by introducing new park

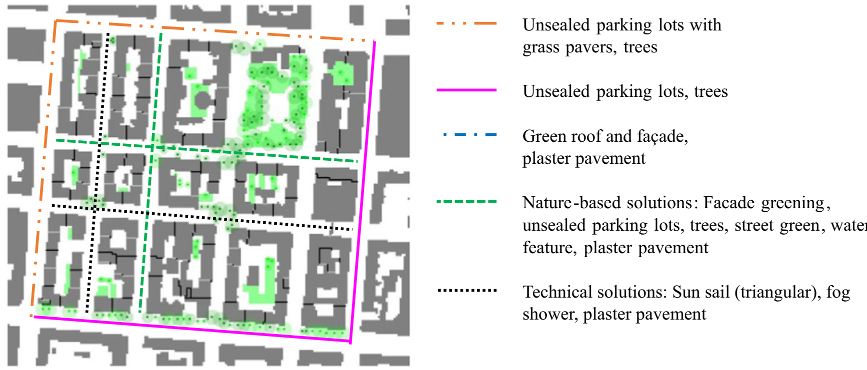

Fig. 6 | Overview of the status quo in the domain "Supergrätzl" in ENVI-Met with designated streets for stated bundles of measures.

Table 5 | Distribution of different land use characteristics

	Micro-scale (Supergrätzl)		City-scale (Densely built-up areas)		Vienna
	Reference	NbS Scenario	Reference	NbS Scenario	Status-Quo
Total	**12.5 ha**		**4068 ha**	**3616 ha**	**41 490[a] ha**
Building area	43.6%	43.6%	42.5% 1728.2 ha	42.6% 1539.9 ha	36%1 14 936.4 ha
Green roof area	0.0%	5.0%	0.0% 0 ha	5% 77 ha	5%[2] 254 ha
Streets/sealed surfaces	53.7%	35.5%	33.9% 1377.3 ha	28.3% 1022.4 ha	15%[1] 6 223.5 ha
Unsealed surface	0.0%	15.2%	12.5% 510.1 ha	15.4% 558.5 ha	not available
Low vegetation and tree trunks	2.7%	5.7%	11.1% 452.4 ha	13.7% 495.3 ha	not available
Number of trees / tree cover	84 trees	231trees	0.2% 9.1 ha	5.1% 207.1 ha	95 997[3] street trees

*Percent of densely built area.
**Street trees relative to reference densely built areas.
***New park area relative to reference densely built areas.
[a]Vienna in figures 2023. https://www.wien.gv.at/statistik/publikationen/wien-in-zahlen.html.
[b]Grünraumanalyse Wien 2010 Dachbegrünung, https://www.wien.gv.at/umweltschutz/raum/pdf/gruenraumanalyse-dachbegruenung.pdf.
[c]Statistisches Jahrbuch der Stadt Wien 2022, https://www.wien.gv.at/statistik/publikationen/jahrbuch.html.

areas for every 9th grid point in the densely built-up areas. The land use change was calculated for each grid point, therefore, the mean spatial values differ to some extent to the micro-scale simulations. Due to the limitations of the MUKLIMO_3 model at lower spatial resolutions, green facades and technical solutions, such as solar sails and water sprays were not considered in the city-scale simulations. Also, water bodies have not been implemented, as they are not present in the densely built-up areas.

Comparing the level of sealed and green surfaces applied in the NbS scenario with the current land use of the whole City of Vienna, it is evident that the current adaptation measures in the densely built-up areas are quantitatively low compared to the total city area. In particular, the green roof potential is underutilized for Vienna as a whole, but the proposed NbS scenario is within the range of current values for the entire city (5% for Vienna as a whole).

A4: Assessing socio-spatial inequalities: Gentrification Trends

As a first step, common to other gentrification studies, we calculated a composite indicator to identify census tracts as gentrified or at risk of gentrification relative to city-wide trends[38,39,86–88]. Following the literature, we calculated decadal change rates for socio-economic characteristics and tenure as indicators of local housing market developments[70,89,90]. Socio-economic and tenure characteristics used include: the proportion of population with compulsory education or a lower education level; proportion of population with university education; change in proportion of unemployed population; proportion of owned apartments; proportion of unregulated private rental dwellings; and proportion of dwellings owned by other legal entities.

Next, we performed a modified shift-share analysis to identify change rates deviating from the city-wide trends for those indicators[91]. The indicators were summarized into a socio-economic upgrading sub-index and a tenure upgrading sub-index. Census tracts at risk of gentrification are classified as those with z-scores of at least one of the sub-indices that are above one standard deviation (1 SD) from the city-wide trend, while the other is still in line with the citywide trends (within -1SD to 1 SD). Tracts are considered gentrified if both sub-indices deviate above one standard deviation. Finally, a binary gentrification index was calculated summing up gentrified tracts and those at risk.

We then tried to identify factors that explain why tracts have gentrified or not based on the above binary gentrification index. This analysis was based on the social-ecological model of gentrification outlined by Rigolon & Németh[87]. The model enables an investigation of which people, place, and policy factors at the beginning of the respective periods predict the odds of gentrification in the following decade. In following this model, we conducted hierarchical logistic regressions for which the statistical requirements were met (see Supplementary Table 3). Multi-collinearity was not detected and all regressions were significant and had moderate explanatory power. Income data are not available at census tract level, therefore this variable had to be omitted from the regression analysis even though it is considered a core characteristic of vulnerability and gentrification.

A5: Assessing socio-spatial inequalities: The role of green surroundings in residential choice

Survey respondents reported on their living situation and on the greenness of their previous, current and prospective future residential location. We controlled for socio-demographic and biographical drivers of residential choice to assess the unique influence of green surroundings. The determination of the role of greenery in residential location choice consisted of two steps.

In the first step, we regressed the greenness of the current residential location on socio-demographic characteristics: change in employment status; changes in household composition; and self-reported satisfaction with green and blue spaces at the previous residential location (Supplementary Table 4). Greenness of the current residential location was operationalized in a first regression model as a mean index of three items from the survey that used a five-step Likert scale from fully agree to fully disagree (Cronbach's $\alpha = 0.77$):

- My urban quarter is greener than most other parts of Vienna;
- Most other parts of Vienna have more green areas and parks than the urban quarter where I live [reverse-coded];
- My urban quarter has more green streets (with trees and bushes) than most other parts of Vienna.

A second regression model used the share of green areas in the current residential district according to the land cadaster as independent variable.

In the second step, we regressed the intention to move from the current residential location on socio-demographic characteristics; characteristics of the current dwelling that may make respondents seek another residence; and the aspiration for green and blue spaces at a prospective future residential location (Supplementary Table 5). Intention to move was operationalized as a mean index of four items using a five-step Likert scale from fully agree to fully disagree ($\alpha = 0.80$):

- 'I have considered to move out of my current place of living';
- 'I am satisfied with my current place of living' [reverse-coded];
- 'I would recommend my current place of living to a good friend' [reverse-coded];
- 'My current place of living satisfies my present needs'[reverse-coded].

To assess the respondent's aspiration for green and blue spaces, they were requested to distribute points over a range of neighborhood characteristics (such as availability of health and childcare amenities, access to transport, access to parks and water bodies). Respondents were asked to distribute 100 points for the current and 120 points for the prospective future residential location, assigning more points to those characteristics they value more.

Predictors entered the hierarchical regression models in two blocks. First, socio-demographic and dwelling characteristics were entered. Second the variables on the aspiration for green and blue spaces were utilized. The differences in the adjusted R^2 values represent the additional variance explained by aspiration for green and blue spaces while correcting for the increasing overall number of predictors.

Reporting summary

Further information on research design is available in the Nature Research Reporting Summary linked to this article.

Data availability

Publicly available data of measured climate data and ÖKS15 projections aggregated to Vienna are available via the websites: https://www.data.gv.at/katalog/dataset/klimadaten-wien; https://public.hub.geosphere.at/public/resources/oks15/timeseries/oks15_timeseries_of_temperature_indices_wien-rcp45-v01/temp-indiceswrcp45.tgz, https://public.hub.geosphere.at/public/resources/oks15/timeseries/oks15_timeseries_of_temperature_indices_wien-rcp85-v01/temp-indiceswrcp85.tgz. Modeled climate data generated by Geosphere Austria are not publicly available, but can be obtained free of cost for research purposes and education. The raw population and dwelling stock data provided by Statistical Department of the City of Vienna and the Austrian Statistical Office are protected and not available. The data on trees from the tree cadaster of Vienna is available at Stadt Wien – data.gv.at: https://www.data.gv.at/katalog/de/dataset/stadt-wien_baumkatasterderstadtwien. The survey data is protected by data privacy laws and is not available. The processed non-proprietary data are available upon reasonable request to the corresponding authors.

Code availability

Code in this study will be made available upon reasonable request.

Received: 22 July 2024; Accepted: 21 February 2025;
Published online: 29 March 2025

References

1. Forster, P. M. et al. Indicators of Global Climate Change 2022: annual update of large-scale indicators of the state of the climate system and human influence. *Earth Syst. Sci. Data* **15**, 2295–2327 (2023).
2. Petzold, J. et al. A global assessment of actors and their roles in climate change adaptation. *Nat. Clim. Change* **13**, 1250–1257 (2023).
3. Manoli, G. et al. Magnitude of urban heat islands largely explained by climate and population. *Nature* **573**, 55–60 (2019).
4. Oke, T. R. City size and the urban heat island. *Atmos. Environ. 1967* **7**, 769–779 (1973).
5. Oke, T. R., Mills, G., Christen, A. & Voogt, J. A. *Urban Climates* (Cambridge University Press, 2017). https://doi.org/10.1017/9781139016476.
6. Elmqvist, T. et al. Urbanization in and for the Anthropocene. *Npj Urban Sustain.* **1**, 1–6 (2021).
7. Chen, M. et al. Rising vulnerability of compound risk inequality to ageing and extreme heatwave exposure in global cities. *Npj Urban Sustain.* **3**, 38 (2023).
8. Gao, J. & Bukovsky, M. S. Urban land patterns can moderate population exposures to climate extremes over the 21st century. *Nat. Commun.* **14**, 6536 (2023).
9. Hsu, A., Sheriff, G., Chakraborty, T. & Manya, D. Disproportionate exposure to urban heat island intensity across major US cities. *Nat. Commun.* **12**, 2721 (2021).
10. Huang, W. T. K. et al. Economic valuation of temperature-related mortality attributed to urban heat islands in European cities. *Nat. Commun.* **14**, 7438 (2023).
11. Intergovernmental Panel On Climate Change (Ipcc). *Climate Change 2022—Impacts, Adaptation and Vulnerability: Working Group II Contribution to the Sixth Assessment Report of the Intergovernmental Panel on Climate Change* (Cambridge University Press, 2023). https://doi.org/10.1017/9781009325844.
12. Lüthi, S. et al. Rapid increase in the risk of heat-related mortality. *Nat. Commun.* **14**, 4894 (2023).
13. Cheng, W., Li, D., Liu, Z. & Brown, R. D. Approaches for identifying heat-vulnerable populations and locations: A systematic review. *Sci. Total Environ.* **799**, 149417 (2021).
14. Ho, H. C., Knudby, A., Chi, G., Aminipouri, M. & Lai, D. Y.-F. Spatiotemporal analysis of regional socio-economic vulnerability change associated with heat risks in Canada. *Appl. Geogr.* **95**, 61–70 (2018).
15. Rosenthal, J. K., Kinney, P. L. & Metzger, K. B. Intra-urban vulnerability to heat-related mortality in New York City, 1997–2006. *Health Place* **30**, 45–60 (2014).
16. Shanahan, D. F., Lin, B. B., Gaston, K. J., Bush, R. & Fuller, R. A. Socio-economic inequalities in access to nature on public and private lands: a case study from Brisbane, Australia. *Landsc. Urban Plan.* **130**, 14–23 (2014).
17. Gabbe, C. J., Mallen, E. & Varni, A. Housing and Urban Heat: Assessing Risk Disparities. *Hous. Policy Debate* **33**, 1078–1099 (2023).
18. Callaghan, A. et al. The impact of green spaces on mental health in urban settings: a scoping review. *J Ment Health* **30**, 179–193 (2021).
19. Jimenez, M. P. et al. Associations between nature exposure and health: a review of the evidence. *Int. J. Environ. Res. Public. Health* **18**, 4790 (2021).
20. Lafortezza, R., Chen, J., Van Den Bosch, C. K. & Randrup, T. B. Nature-based solutions for resilient landscapes and cities. *Environ. Res.* **165**, 431–441 (2018).
21. Marando, F. et al. Urban heat island mitigation by green infrastructure in European Functional Urban Areas. *Sustain. Cities Soc.* **77**, 103564 (2022).
22. Cameron, R. W. F. et al. The domestic garden – Its contribution to urban green infrastructure. *Urban For. Urban Green.* **11**, 129–137 (2012).

23. Chen, W. Y., Liekens, I. & Broekx, S. Identifying societal preferences for river restoration in a densely populated urban environment: evidence from a discrete choice experiment in Central Brussels. *Environ. Manage.* **60**, 263–279 (2017).
24. Ebenberger, M. & Arnberger, A. Exploring visual preferences for structural attributes of urban forest stands for restoration and heat relief. *Urban For. Urban Green.* **41**, 272–282 (2019).
25. Norton, B. A. et al. Planning for cooler cities: A framework to prioritise green infrastructure to mitigate high temperatures in urban landscapes. *Landsc. Urban Plan.* **134**, 127–138 (2015).
26. Matthews, T., Lo, A. Y. & Byrne, J. A. Reconceptualizing green infrastructure for climate change adaptation: Barriers to adoption and drivers for uptake by spatial planners. *Landsc. Urban Plan.* **138**, 155–163 (2015).
27. Sprondel, N., Donner, J., Mahlkow, N. & Köppel, J. Urban climate and heat stress: how likely is the implementation of adaptation measures in mid-latitude cities? The case of façade greening analyzed with Bayesian networks. *One Ecosyst.* **1**, e9280 (2016).
28. Johnson, D., See, L., Oswald, S. M., Prokop, G. & Krisztin, T. A cost–benefit analysis of implementing urban heat island adaptation measures in small- and medium-sized cities in Austria. *Environ. Plan. B: Urban Anal. City Sci.* **48**, 2326–2345 (2021).
29. Nesshöver, C. et al. The science, policy and practice of nature-based solutions: An interdisciplinary perspective. *Sci. Total Environ.* **579**, 1215–1227 (2017).
30. Ommer, J. et al. Quantifying co-benefits and disbenefits of Nature-based Solutions targeting Disaster Risk Reduction. *Int. J. Disaster Risk Reduct.* **75**, 102966 (2022).
31. Kabisch, N. et al. Nature-based solutions to climate change mitigation and adaptation in urban areas: perspectives on indicators, knowledge gaps, barriers, and opportunities for action. *Ecol. Soc*. **21** (2016).
32. Perkins, H. A., Heynen, N. & Wilson, J. Inequitable access to urban reforestation: the impact of urban political economy on housing tenure and urban forests. *Cities* **21**, 291–299 (2004).
33. Keeler, B. L. et al. Social-ecological and technological factors moderate the value of urban nature. *Nat. Sustain.* **2**, 29–38 (2019).
34. Shi, L. et al. Roadmap towards justice in urban climate adaptation research. *Nat. Clim. Change* **6**, 131–137 (2016).
35. Chakraborty, T., Hsu, A., Manya, D. & Sheriff, G. Disproportionately higher exposure to urban heat in lower-income neighborhoods: a multi-city perspective. *Environ. Res. Lett.* **14**, 105003 (2019).
36. Rocha, A. D. et al. Unprivileged groups are less served by green cooling services in major European urban areas. *Nat. Cities* **1**, 424–435 (2024).
37. Chu, E. K. & Cannon, C. E. Equity, inclusion, and justice as criteria for decision-making on climate adaptation in cities. *Curr. Opin. Environ. Sustain.* **51**, 85–94 (2021).
38. Anguelovski, I. et al. Green gentrification in European and North American cities. *Nat. Commun.* **13**, 3816 (2022).
39. Quinton, J., Nesbitt, L., Connolly, J. J. & Wyly, E. How common is greening in gentrifying areas? *Urban Geogr.* **45**, 1–23 (2023).
40. Nijman, J. & Wei, Y. D. Urban inequalities in the 21st century economy. *Appl. Geogr.* **117**, 102188 (2020).
41. García-Lamarca, M., Anguelovski, I. & Venner, K. Challenging the financial capture of urban greening. *Nat. Commun.* **13**, 7132 (2022).
42. Sarabi, S. et al. Uptake and implementation of Nature-Based Solutions: An analysis of barriers using Interpretive Structural Modeling. *J. Environ. Manage.* **270**, 110749 (2020).
43. Kauark-Fontes, B., Marchetti, L. & Salbitano, F. Integration of nature-based solutions (NBS) in local policy and planning toward transformative change. Evidence from Barcelona, Lisbon, and Turin. *Ecol. Soc*. **28** (2023).
44. Frantzeskaki, N. et al. in *Nature-Based Solutions for* Cities Ch. 11 (eds. McPhearson, T., Kabisch, N. & Frantzeskaki, N.) 241–258 (Edward Elgar Publishing, 2023).
45. Di Marino, M., Cucca, R., Thaler, T. & Bügelmayer-Blaschek, M. Interlinking the silos: How to stimulate a new debate on more greenery in cities. *Urban For. Urban Green* **87**, 128065 (2023).
46. European Environment Agency. Towards 'just resilience': leaving no one behind when adapting to climate change https://www.eea.europa.eu/publications/just-resilience-leaving-no-one-behind/towards-just-resilience-leaving-no (2022).
47. Olefs, M. et al. Past and future changes of the Austrian climate—importance for tourism. *J. Outdoor Recreat. Tour.* **34**, 100395 (2021).
48. Stadt Wien. Klimadaten Wien - data.gv.at.
49. CCCA Data Centre. ÖKS15 Timeseries of Temperature Indices: Wien - rcp4.5 (2016).
50. CCCA Data Centre. ÖKS15 Timeseries of Temperature Indices: Wien - rcp8.5 (2016).
51. Chimani, B. Endbericht ÖKS15 – Klimaszenarien für Österreich - Daten - Methoden - Klimaanalyse. GeoSphere Austria https://doi.org/10.60669/WGXM-4927 (2018).
52. Sievers, U. *Das Kleinskalige Strömungsmodell MUKLIMO_3*. 155 (2016).
53. Reinwald, F. et al. Multi-level toolset for steering urban green infrastructure to support the development of climate-proofed cities. *Sustainability* **13**, 12111 (2021).
54. Jacob, D. et al. EURO-CORDEX: new high-resolution climate change projections for European impact research. *Reg. Environ. Change* **14**, 563–578 (2014).
55. Bokwa, A. et al. Urban climate in Central European cities and global climate change. *Acta Climatol. Chorol* **51–52**, 7–35 (2018).
56. Früh, B. et al. Estimation of climate-change impacts on the urban heat load using an urban climate model and regional climate projections. *J. Appl. Meteorol. Climatol* **50**, 167–184 (2011).
57. Karl, T. R., Nicholls, N. & Ghazi, A. Clivar/GCOS/WMO Workshop on Indices and Indicators for Climate Extremes Workshop Summary. *Clim. Change* **42**, 3–7 (1999).
58. Moss, R. H. et al. The next generation of scenarios for climate change research and assessment. *Nature* **463**, 747–756 (2010).
59. Stocker, T. *Climate Change 2013: The Physical Science Basis: Working Group I Contribution to the Fifth Assessment Report of the Intergovernmental Panel on Climate Change* (Cambridge University Press, 2014).
60. Schumacher, D. L. et al. Exacerbated summer European warming not captured by climate models neglecting long-term aerosol changes. *Commun. Earth Environ.* **5**, 1–14 (2024).
61. Statistik Austria. STATcube - Statistische Datenbank (2024).
62. Dellink, R., Chateau, J., Lanzi, E. & Magné, B. Long-term economic growth projections in the Shared Socioeconomic Pathways. *Glob. Environ. Change* **42**, 200–214 (2017).
63. Kc, S. & Lutz, W. The human core of the shared socioeconomic pathways: Population scenarios by age, sex and level of education for all countries to 2100. *Glob. Environ. Change* **42**, 181–192 (2017).
64. Rao, N. D., Sauer, P., Gidden, M. & Riahi, K. Income inequality projections for the Shared Socioeconomic Pathways (SSPs). *Futures* **105**, 27–39 (2019).
65. Riahi, K. et al. The Shared Socioeconomic Pathways and their energy, land use, and greenhouse gas emissions implications: An overview. *Glob. Environ. Change* **42**, 153–168 (2017).
66. ÖROK. ÖROK-Bevölkerungsprognose 2021. https://www.oerok.gv.at/raum/daten-und-grundlagen/oerok-prognosen/oerok-prognose-2021-1 (2021).
67. European Commission, Eurostat. At-risk-of-poverty rate by degree of urbanisation (2024).
68. European Commission, Eurostat. Population by educational attainment level, sex, age, country of birth and degree of urbanisation (%). (2024).

69. Stadt Wien. Baumkataster bzw. Bäume Standorte Wien. https://www.data.gv.at/katalog/de/dataset/stadt-wien_baumkatasterderstadtwien (2022).
70. Kadi, J. & Matznetter, W. The long history of gentrification in Vienna, 1890–2020. *City* **26**, 450–472 (2022).
71. Mazziotta, M. & Pareto, A. Data normalization for aggregating time series: the constrained min-max method. *Rivista Italiana di Economia Demografia e Stastica* **LXXV**, 101–108 (2021).
72. O'Neill, B. C. et al. The roads ahead: Narratives for shared socioeconomic pathways describing world futures in the 21st century. *Glob. Environ. Change* **42**, 169–180 (2017).
73. Frigerio, I., Carnelli, F., Cabinio, M. & De Amicis, M. Spatiotemporal Pattern of Social Vulnerability in Italy. *Int. J. Disaster Risk Sci.* **9**, 249–262 (2018).
74. Santos, P. P., Zêzere, J. L., Pereira, S., Rocha, J. & Tavares, A. O. A Novel Approach to Measuring Spatiotemporal Changes in Social Vulnerability at the Local Level in Portugal. *Int. J. Disaster Risk Sci.* **13**, 842–861 (2022).
75. Lancaster, K. J. A new approach to consumer theory. *J. Polit. Econ.* **74**, 132–157 (1966).
76. McFadden, D. Conditional logit analysis of qualiatative choice behaviour. In *Frontiers in Econometrics*, Zarembka, P. (ed), pp. 105–142 (Academic Press, New York, 1974).
77. Sobol', I. M. On the distribution of points in a cube and the approximate evaluation of integrals. *USSR Comput. Math. Math. Phys.* **7**, 86–112 (1967).
78. Owen, A. B. in *Monte Carlo and Quasi-Monte Carlo Methods in Scientific Computing* (eds. Niederreiter, H. & Shiue, P. J.-S.) 106, 299–317 (Springer New York, 1995).
79. Faure, H. & Tezuka, S. in *Monte Carlo and Quasi-Monte Carlo Methods 2000* (eds. Fang, K.-T., Niederreiter, H. & Hickernell, F. J.) 242–256 (Springer Berlin Heidelberg, 2002). https://doi.org/10.1007/978-3-642-56046-0_16.
80. Czajkowski, M. & Budziński, W. Simulation error in maximum likelihood estimation of discrete choice models. *J. Choice Model.* **31**, 73–85 (2019).
81. Krinsky, I. & Robb, A. L. Three methods for calculating the statistical properties of elasticities: a comparison. *Empir. Econ.* **16**, 199–209 (1991).
82. Bliemer, M. C. J. & Rose, J. M. Confidence intervals of willingness-to-pay for random coefficient logit models. *Transp. Res. B: Methodol.* **58**, 199–214 (2013).
83. Hole, A. R. A comparison of approaches to estimating confidence intervals for willingness to pay measures. *Health Econ.* **16**, 827–840 (2007).
84. Albdour, M. S. & Baranyai, B. An overview of microclimate tools for predicting the thermal comfort, meteorological parameters and design strategies in outdoor spaces. *Pollack Period* **14**, 109–118 (2019).
85. Bruse, M. ENVI-met Version 5.0. https://envi-met.com/ (2022).
86. Anguelovski, I., Connolly, J. J. T., Masip, L. & Pearsall, H. Assessing green gentrification in historically disenfranchised neighborhoods: a longitudinal and spatial analysis of Barcelona. *Urban Geogr.* **39**, 458–491 (2018).
87. Rigolon, A. & Németh, J. Toward a socioecological model of gentrification: How people, place, and policy shape neighborhood change. *J. Urban Aff.* **41**, 887–909 (2019).
88. Rigolon, A. & Németh, J. Green gentrification or 'just green enough': Do park location, size and function affect whether a place gentrifies or not? *Urban Stud.* **57**, 402–420 (2020).
89. Musil, R., Brand, F., Huemer, H. & Wonaschütz, M. The Zinshaus market and gentrification dynamics: The transformation of the historic housing stock in Vienna, 2007–2019. *Urban Stud* **59**, 974–994 (2022).
90. Banabak, S. Neighbourhood rental market integration and private rent trajectories—evidence from the city of Vienna. *Int. J. Urban Sci.* **27**, 239–259 (2023).
91. Holm, A. & Schulz, G. in *Gentrification and Resistance: Researching Displacement Processes and Adaption Strategies* (ed. Helbrecht, I.) 251–277 (Springer Fachmedien, 2018). https://doi.org/10.1007/978-3-658-20388-7_10.

Acknowledgements

This study was funded by the Vienna Science and Technology Fund (WWTF) [10.47379/ESR20011] within the SENSUS project "The social equality of Nature-based Solutions to urban heat stress".

Author contributions

Conceptualization: M.F., A.S., T.T., M.G., S.S., M.B.B. M.Z.A.; Data collection: M.F., C.H., M.Z.A., M.S.; Data analysis: M.F., W.Z., M.Z.A., S.S., M.B.B., A.S., M.S.; Interpretation of Results: M.F., A.S., W.Z., C.H., M.Z.A., S.S., M.S., M.B.B.; Writing—Original Draft: M.F., A.S., C.H., M.Z.A., S.S., M.B.B., M.S., T.T.; Writing—Review and Editing: M.F., A.S., C.H., M.Z.A., S.S., M.B.B., W.Z., M.S., M.G., T.T.; Visualization: M.F., A.S., M.S.; Supervision: T.T., M.G.; Funding acquisition: T.T., M.G., M.Z.A.

Competing interests

The authors declare no competing interests.

Additional information

Supplementary information The online version contains supplementary material available at https://doi.org/10.1038/s42949-025-00202-2.

Correspondence and requests for materials should be addressed to Michael Friesenecker or Antonia Schneider.